

Metal-insulator transitions in epitaxial LaVO_3 and LaTiO_3 films

C. He,^{1,*} T. D. Sanders,¹ M. T. Gray,¹ F. J. Wong,^{1,†} V. V. Mehta,^{1,2} and Y. Suzuki^{1,2,3}

¹*Department of Materials Science and Engineering, University of California, Berkeley, California 94720*

²*Materials Sciences Division, Lawrence Berkeley National Laboratory, Berkeley, California 94720*

³*Department of Applied Physics and Geballe Laboratory for Advanced Materials, Stanford University, Stanford, California 94305*

(Received 17 April 2012; revised manuscript received 7 June 2012; published 1 August 2012)

We have demonstrated that epitaxial films of LaVO_3 and LaTiO_3 can exhibit metallicity though their bulk counterparts are Mott insulators. When LaTiO_3 films are compressively strained on SrTiO_3 substrates, we observe metallicity that is attributed largely to epitaxial strain-induced electronic structure modifications and secondarily to interface electronic reconstruction at the $\text{LaTiO}_3/\text{SrTiO}_3$ interface. However, when LaVO_3 films are compressively strained on SrTiO_3 substrates, the observed metallicity is primarily attributed to interface effects. Signatures of weak localization are observed at low temperature in LaVO_3 films in the temperature, film thickness, as well as magnetic field dependence of the magnetoresistance.

DOI: [10.1103/PhysRevB.86.081401](https://doi.org/10.1103/PhysRevB.86.081401)

PACS number(s): 73.61.-r, 71.30.+h, 72.80.Ga

Metal-insulator transitions have been intensively studied in many condensed matter systems.¹ In these systems, external parameters such as temperature and electric or magnetic field push the system from an insulating to metallic state or vice versa. More recently, the generation of metallic ground states in epitaxial heterostructures—composed of materials which are insulating in the bulk—has led to an explosion of research activity in perovskite transition-metal oxide heterostructures. The most well-known examples are $\text{LaAlO}_3/\text{SrTiO}_3$ (LAO/STO)² and LaTiO_3 (LTO)/STO.^{3,4} It is now generally agreed upon that the metallicity at the interface of the two band insulators LAO and STO is attributed to a polar discontinuity at the interface if the materials are well oxygenated.⁵ In LTO/STO, some believe that the metallicity at this Mott insulator/band insulator interface is due to an electronic reconstruction at the interface,^{3,4} while others ascribe the metallicity primarily to lattice-induced electronic structure modification.^{6,7} In analogy with the LTO/STO system, Hotta *et al.* have also studied LaVO_3/STO (LVO/STO) and again attributed metallicity to interface electronic reconstruction.⁸ However, other polar-nonpolar interfaces, such as $\text{LaMnO}_3/\text{STO}$ and $\text{LaCrO}_3/\text{STO}$, are not metallic.^{9,10} Both LTO/STO and LVO/STO systems not only provide polar-nonpolar interfaces but also have small insulating gaps and orbital degrees of freedom (t_{2g}^1 and t_{2g}^2) that may be linked to a metal-insulator transition. With advances in thin-film deposition techniques, we have unprecedented control of these interfaces and there is no doubt that interface electronic reconstruction plays a role in the generation of metallicity. However, other interface effects, such as screening due to high dielectric constant materials, as well as epitaxial strain-induced modification of the electronic structure must also be carefully taken into account.

In order for epitaxial strains to induce enough lattice distortion to modify the electronic structure, the charge gap in the strained compound must be relatively small. In the bulk, the Mott insulating gap in LTO is ~ 0.1 eV, while that in LVO is ~ 1.1 eV.¹¹ Despite the similar lattice parameters of the two compounds, the order-of-magnitude difference in the gap suggests that the origin of the observed metallicity may be very different in LTO/STO and LVO/STO.

In this Rapid Communication, we demonstrate that the metallic ground state in LVO/STO is qualitatively different from that in LTO/STO. In LTO/STO, the metallic state is found in the bulk of the LTO film and not just at the interface with STO. We demonstrate that the metallicity of LTO/STO is attributed to a combination of the effects of strain-induced electronic structure modifications and interface effects. This result reconciles previous contradictory reports on the origin of the metallicity. The small Mott insulating gap likely can be collapsed by the 1.67% epitaxial mismatch strain imposed by the underlying STO substrate. Previous *ab initio* studies with dynamical mean-field modeling suggest that lattice distortions can indeed stabilize a metallic ground state in LTO.⁶ The larger gap in LVO cannot be collapsed by lattice distortions alone. Metallicity is induced at the interface as is evident in the scaling of the sheet resistivity in LVO films of varying thicknesses grown on STO. A comparison of the low-temperature transport behavior of the metallic ground state in LVO/STO and LTO/STO also suggests the different origins of the metallicity. In LTO/STO, there is a precipitous drop in the resistivity at low temperatures. In LVO/STO, the low-temperature upturn in resistivity shows signatures of weak localization. Moreover, the in-plane magnetoresistance (MR) shows a local maximum that is associated with strong spin-orbit coupling in the system as a result of the competition between weak localization and antilocalization in the presence of an external magnetic field.

Single films and bilayers of LTO and LVO were fabricated via pulsed laser deposition with a KrF laser (wavelength of $\lambda = 248$ nm and laser fluence of ~ 1.4 J/cm²) at 625 °C and frequency of 3 Hz using $\text{La}_2\text{Ti}_2\text{O}_7$ and LaVO_4 targets, respectively. Ohtomo *et al.* have found that pulsed laser deposition can stabilize the LaTiO_3 phase starting from an oxygen-rich $\text{La}_2\text{Ti}_2\text{O}_7$ target, the more readily achievable bulk stoichiometry.¹² Hotta *et al.* have found that LaVO_3 films can be stabilized in reduced partial pressures of oxygen at 500–900 °C from a LaVO_4 target.¹³ LTO films were grown in 10^{-6} Torr and LVO films were grown in 10^{-6} (or 10^{-5}) Torr, as specified later. The bulk average pseudocubic lattice parameter of LTO is ~ 3.97 Å and of LVO is ~ 3.93 Å. In this paper, we will use pseudocubic indices for plane and direction

notation. These films were grown 15–85 nm thick on various substrates, including STO ($a = 3.905 \text{ \AA}$) and DyScO_3 (DSO is orthorhombic with pseudocubic lattice parameter $\sim 3.942 \text{ \AA}$). In addition, LTO and LVO films were grown on STO buffered DSO and LTO/LVO bilayers were grown on STO and DSO substrates. X-ray diffraction (XRD) experiments in the form of θ - 2θ scans, x-ray reflectivity (XRR), and reciprocal space maps (RSM) were performed on an X'Pert Panalytical MRD system. All resistivity measurements and Hall measurements were performed on a Quantum Design Physical Properties Measurement System with applied fields up to 70 kOe and in temperatures down to 2 K.

Structural characterization of the samples indicates that all the samples have excellent crystallinity with $\Delta\omega \sim 0.13$ – 0.19° , as determined by XRD θ - 2θ scans. RSM measurements of the single films and bilayers indicate that all samples are coherently strained to the substrate and result in tetragonal symmetry in the films.⁷ In particular, all LTO films are compressively strained to the underlying substrates with -0.7% for DSO and -1.6% for STO. LVO films are tensilely strained on DSO (0.31%) and compressively strained on STO (-0.64%). It turns out that the sign of the strain has no direct correlation with the conductivity as is demonstrated later. Sample thickness values were determined via XRR.

Transport measurements of the single and bilayer films together provide a compelling picture explaining the metallicity in LVO and LTO films. Figure 1(a) shows 28-nm-thick LTO films grown at the same time on STO and DSO substrates, while Fig. 1(b) shows 28-nm-thick LVO films grown at the same time on STO and DSO. These resistivity versus temperature measurements reveal metallic behavior in compressively strained LTO on STO and insulating behavior

in compressively strained LTO on DSO. Our previous study of LTO films on STO, DSO, and GdScO_3 substrates demonstrates that larger coherent compressive strain corresponds to lower resistivity (i.e., metallic LTO on STO, semiconducting LTO on DSO, and bulklike insulating LTO on GSO).⁷ Likewise LVO films on STO are metallic, while LVO films on DSO are insulating.

When we insert a thin LVO buffer layer (3 nm) between the LTO films and STO or DSO substrates, we observe metallic and insulating behavior, respectively, that can be explained in terms of lattice-induced electronic structure modification [Fig. 1(a)]. However, when LTO films are grown on STO (6.7 nm) buffered DSO, we observe metallic behavior although not as conducting as LTO films grown directly on STO substrates. If lattice-induced electronic structure modifications were the only source of metallicity, LTO films grown on STO buffered DSO should exhibit insulating behavior similar to LTO films grown directly on DSO substrates. Clearly the metallic behavior in LTO/STO/DSO samples suggests that interface effects, including possible polar discontinuity or dielectric screening due to the STO substrate, also contribute to the overall metallic behavior of LTO films, albeit to a lesser degree. Therefore the small Mott insulating gap $\sim 0.1 \text{ eV}$ of LTO¹¹ is collapsed by lattice distortions associated with epitaxial strain on a STO substrate combined with other factors associated with the interface, such as polar discontinuity,⁸ and can induce a transition from an insulator to a metal. These conclusions reconcile previous contradictory explanations where the metallicity of LTO/STO superlattices has been associated with charge transfer at the interface⁴ and the metallicity of LTO films on STO substrates has been associated with a bulk film effect.^{6,7}

For LVO, which has a larger Mott insulating gap of $\sim 1.1 \text{ eV}$ ¹¹ in the bulk, a metal-insulator transition appears to be accessible in thin film form. In order to determine the origin of the metallicity, we studied epitaxial LVO films grown coherently on DSO substrates and STO buffered DSO substrates (LVO/STO/DSO), as well as films grown on STO substrates. Figure 1(b) shows the transport properties of these LVO films. The LVO films grown on STO substrates exhibit metallic behavior albeit with a weaker temperature dependence compared to the corresponding LTO films. It is worthwhile to point out that such metallicity is not due to oxygen defects in STO since a bare STO exposed to the same growth conditions, but without actual deposition of an LVO film, is too insulating to be measured. The resistivity curves of the LVO/STO samples over a 10–300 K range are in agreement with earlier reports by Hotta *et al.*⁸ In their study, the metallicity was attributed to polar discontinuity, similar to LAO/STO.² Our LVO/DSO samples show insulating behavior, as expected, since LVO is closely lattice matched to DSO. In order to determine whether metallicity in LVO/STO is attributed to lattice-induced electronic structure modifications or the LVO/STO interface, we studied LVO/STO/DSO composed of a LVO/STO bilayer that is coherently strained to DSO. Basically this sample possesses the same interface, and therefore the same polar discontinuity as LVO/STO, while having the same degree of strain as LVO/DSO. If polar discontinuity dictates the transport behavior, we expect that LVO/STO/DSO should be metallic just like LVO/STO. However, if strain dominates

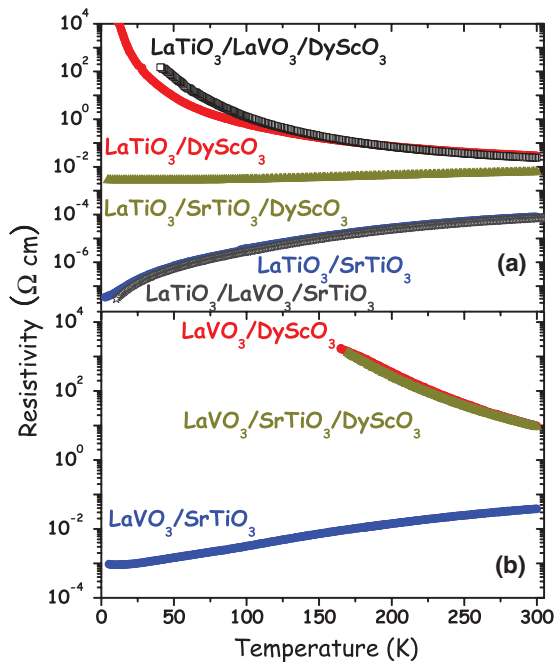


FIG. 1. (Color online) Temperature dependence of resistivity in zero field of (a) LaTiO_3 films and bilayers grown on SrTiO_3 and DyScO_3 , and (b) LaVO_3 films and bilayers grown on SrTiO_3 and DyScO_3 .

the transport properties, one would expect LVO/STO/DSO to be insulating. Figure 1(b) shows that LVO/STO/DSO is insulating and matches the behavior of LVO/DSO. As a side note, the agreement in resistivity between LVO/DSO and LVO/STO/DSO is independent of oxygen growth pressures ranging from 10^{-5} to 10^{-6} Torr. Furthermore, all LVO samples grown on STO substrates or buffer layers had TiO_2 termination and showed transport behavior identical to those samples which were not TiO_2 terminated.

In order to determine whether the origin of the metallicity in LVO/STO is a bulk film effect or an interface effect, LVO films with different thicknesses (15, 28, and 85 nm) were grown on STO substrates. In contrast to the thickness dependence of LTO films where the three-dimensional resistivity was constant for all coherently strained LTO films on STO,⁷ the sheet resistance values of the LVO films on STO are constant from 100 to 300 K for all coherently strained films as shown in Fig. 2. The upturn in resistivity at low temperatures (2–100 K), which we believe comes from weak localization, will be discussed later. The thickness-independent sheet resistance at higher temperature suggests that the metallic behavior is limited to the interfaces. Hall-effect measurements indicate the carriers to be electrons as in LTO films.⁷ The sheet carrier concentration n_{2D} values of all films are also similar to a temperature dependence that suggests carrier saturation at higher temperatures (Fig. 2, inset). These sheet carrier concentration values are consistent with those determined by other groups.^{8,14} The mobility and its temperature dependence of LVO/STO samples (Fig. 2, inset) indicate that it is dominated by impurities at low temperatures and phonons at higher temperatures similar to both LAO/STO and LTO/STO. All of these observations are at odds with the lattice-induced electronic structure modification argument, where the metallicity is a bulk film effect and not limited to the interface.

In order to explain both the thickness dependence of the LVO/STO samples and the transport behavior of LVO/STO, LVO/DSO, and LVO/STO/DSO samples, we must attribute the metallicity to an interface effect. One possible explanation for the metallicity is the dielectric screening of the carriers in LVO due to the dramatic increase in dielectric constant of STO

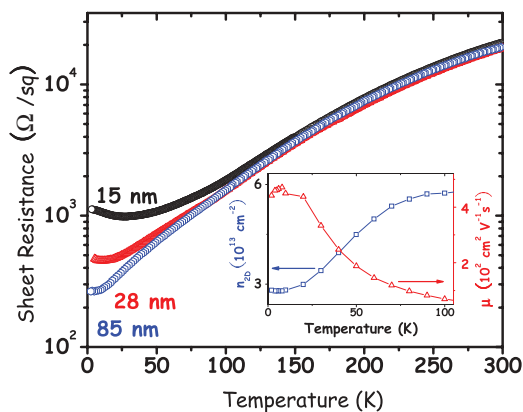


FIG. 2. (Color online) Temperature dependence in zero field of sheet resistance of $\text{LaVO}_3/\text{SrTiO}_3$ films (15 nm, 28 nm, 85 nm). Inset: Sheet carrier concentrations as well as Hall mobility of 28 nm film from 2 to 105 K.

at low temperatures.¹⁵ Dielectric screening is likely a factor in LTO/STO samples, as well as LAO/STO,¹⁶ especially at low temperatures where the dielectric constant of STO increases dramatically. In LVO/STO/DSO films, the 6.7-nm-thick STO buffer layer may not be sufficiently thick to generate the same dielectric screening effect as an STO substrate, thus giving rise to insulating behavior.

Another possible explanation for the metallicity of LVO films is a polar discontinuity at the LVO/STO interface as suggested by Hotta *et al.*⁸ Metallic behavior induced by a polar discontinuity at the LVO/STO interface may be dramatically modified if the STO is strained in the form of a buffer layer. The strain may be enough to modify the electronic structure in STO and, in turn, localize the carriers transferred into STO from the Mott insulator LVO in LVO/STO/DSO films.

To probe the origin of the upturn in resistivity at low temperature in LVO/STO films, we performed both in-plane (IP) and out of plane (OOP) magnetoresistance (MR) measurements. The temperature dependence of OOP MR of the 28-nm film is shown in Fig. 3(a). Positive MR is seen at low temperatures. Quantitative analysis shows the quadratic dependence of MR on field at fixed temperature and the quadratic dependence of the MR on mobility at fixed field. Together these results indicate that the observed positive MR is due to orbital effects and obeys Kohler's rule.¹⁷

The IP MR, however, shows distinctly different behavior in the same temperature range, as shown in Fig. 3(b). Negative MR is seen at 10 K and appears to be a signature of weak localization to which all 2D materials with any degree of

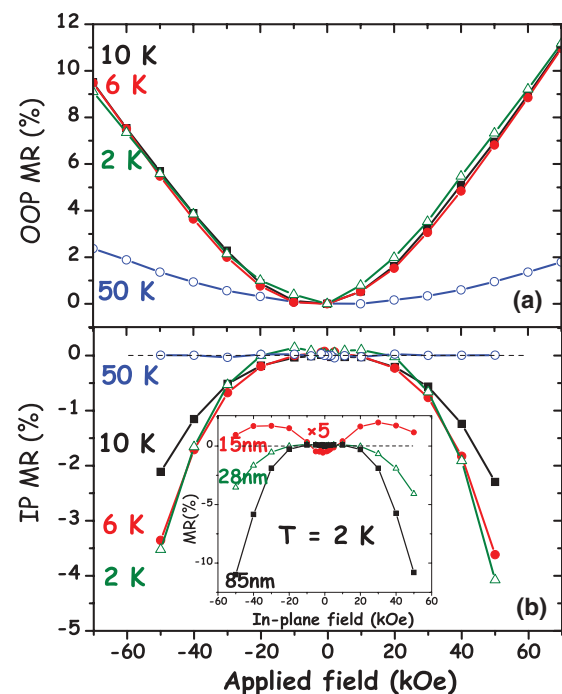


FIG. 3. (Color online) Field dependence of (a) out-of-plane magnetoresistance (OOP MR) and (b) in-plane magnetoresistance (IP MR) of the $\text{LaVO}_3/\text{SrTiO}_3$ film (28 nm) at $T = 2, 6, 10,$ and 50 K. Inset of (b): In-plane magnetoresistance of the $\text{LaVO}_3/\text{SrTiO}_3$ films (15, 28, and 85 nm) at $T = 2$ K.

disorder are susceptible.¹⁸ Weak localization is the quantum manifestation of enhanced backscattering interference,^{19,20} which can be modified by an external magnetic field. At 2 K [Fig. 3(b), inset], MR is positive at low fields and becomes negative at larger fields, thereby producing a local maximum in MR. Such a local maximum may be a manifestation of the competition of weak localization and weak antilocalization in the presence of an external magnetic field and usually exists in a system with strong spin-orbit coupling,^{19,20} such as the well-known Au-doped Mg films.²¹ The local maximum shifts to lower field and eventually vanishes with increasing temperature. The disappearance of the local maximum corresponds to the decrease in inelastic scattering time below the spin-orbit scattering time with increasing temperature. Similar trends have also been observed in bismuth films.²²

In summary, by comparing the transport properties of the films of two bulk Mott insulators LTO (bulk gap 0.1 eV) and LVO (bulk gap 1.1 eV), we have shown that the gap in LTO can be collapsed in the bulk of the film with epitaxial strain, while metallicity in LVO is limited to the interface

with STO. The metallicity observed in LTO film grown on buffered STO/DSO suggests a secondary contribution from the polar discontinuity at the interface. However, the metallic behavior of our LVO/STO films is not primarily due to a lattice-induced electronic structure modification. Its thickness independence of sheet resistance suggests that the metallicity is interfacial in nature and likely due to polarity discontinuity. In addition, the LVO/STO films show signatures of weak localization that is observed in other two-dimensional metallic systems with strong spin-orbit coupling. Together these results indicate that epitaxial strain, polar discontinuity, and dielectric screening effects must be duly taken into consideration when interpreting metallic behavior in these complex oxide heterostructures.

This work is supported by the Director, Office of Science, Office of Basic Energy Sciences, of the US Department of Energy (DOE) (DE-AC02-05CH11231). F.J.W. and M.T.G. were supported by the Army Research Office MURI-W911 NF-08-1-0317.

*chunyong.he@gmail.com

†Present address: School of Engineering and Applied Sciences, Harvard University, Cambridge, MA 02138.

¹M. Imada, M. Fujimori, and Y. Tokura, *Rev. Mod. Phys.* **70**, 4 (1998).

²A. Ohtomo and H. Y. Hwang, *Nature (London)* **427**, 423 (2004).

³A. Ohtomo, D. A. Muller, J. L. Grazul, and H. Y. Hwang, *Nature (London)* **419**, 378 (2002).

⁴K. Shibuya, T. Ohnishi, M. Kawasaki, H. Koinuma, and M. Lippmaa, *Jpn. J. Appl. Phys.* **43**, L1178 (2004).

⁵M. Huijben, A. Brinkman, G. Koster, G. Rijnders, H. Hilgenkamp, and D. H. A. Blank, *Adv. Mater.* **21**, 1665 (2009).

⁶H. Ishida and A. Liebsch, *Phys. Rev. B* **77**, 115350 (2008).

⁷F. J. Wong, S. H. Baek, R. V. Chopdekar, V. V. Mehta, H. W. Jang, C. B. Eom, and Y. Suzuki, *Phys. Rev. B* **81**, 161101(R) (2010).

⁸Y. Hotta, T. Susaki, and H. Y. Hwang, *Phys. Rev. Lett.* **99**, 236805 (2007).

⁹S. A. Chambers, L. Qiao, T. C. Droubay, T. C. Kaspar, B. W. Arey, and P. V. Sushko, *Phys. Rev. Lett.* **107**, 206802 (2011).

¹⁰P. Perna, D. Maccariello, M. Radovic, U. Scott di Uccio, I. Pallecchi, M. Codda, D. Marre, C. Cantoni, J. Gazquez, M. Varela, S. J. Pennycook, and F. Miletto Granozio, *Appl. Phys. Lett.* **97**, 152111 (2010).

¹¹T. Arima, Y. Tokura, and J. B. Torrance, *Phys. Rev. B* **48**, 17006 (1993).

¹²A. Ohtomo, D. A. Muller, J. L. Grazul, and H. Y. Hwang, *Appl. Phys. Lett.* **80**, 3922 (2002).

¹³Y. Hotta, Y. Mukunoki, T. Susaki, H. Y. Hwang, L. Fitting, and D. A. Muller, *Appl. Phys. Lett.* **89**, 031918 (2006).

¹⁴S. Miyasaka, T. Okuda, and Y. Tokura, *Phys. Rev. Lett.* **85**, 5388 (2000).

¹⁵T. Sakudo and H. Unoki, *Phys. Rev. Lett.* **24**, 851 (1971).

¹⁶W. Siemons, M. Huijben, G. Rijnders, D. H. A. Blank, T. H. Geballe, M. R. Beasley, and G. Koster, *Phys. Rev. B* **81**, 241308 (2010).

¹⁷Kohlers rule $MR = F(H/\rho) \approx F'(\mu H)$, where H is the magnetic field, ρ is the sample resistivity, and F and F' are monotonic functions.

¹⁸F. J. Wong, R. V. Chopdekar, and Y. Suzuki, *Phys. Rev. B* **82**, 165413 (2010).

¹⁹G. Bergmann, *Phys. Rep.* **107**, 1 (1984).

²⁰S. Wang and P. E. Lindelof, *J. Low Temp. Phys.* **71**, 403 (1988).

²¹G. Bergmann, *Phys. Rev. Lett.* **48**, 1046 (1982).

²²Yu. F. Komnik, V. V. Andrievskii, and I. B. Berkutov, *Low Temp. Phys.* **33**, 79 (2007).